Nucleation at hardness indentations in cold rolled Al

Xu, C.L.; Zhang, Yubin; Wu, G.L.; Liu, Q.; Juul Jensen, Dorte

Published in:
I O P Conference Series: Materials Science and Engineering

Link to article, DOI:
10.1088/1757-899X/89/1/012054

Publication date:
2015

Document Version
Publisher's PDF, also known as Version of record

Nucleation at hardness indentations in cold rolled Al

2015 IOP Conf. Ser.: Mater. Sci. Eng. 89 012054

(http://iopscience.iop.org/1757-899X/89/1/012054)

Nucleation at hardness indentations in cold rolled Al

C L Xu[1, 2], Y B Zhang[2], G L Wu[1], Q Liu[1], D Juul Jensen[2]

[1] College of Material Science and Engineering, Chongqing University, Chongqing 400044, China
[2] Danish-Chinese Center for Nanometals, Section for Materials Science and Advanced Characterization, Department of Wind Energy, Technical University of Denmark, Risø Campus, DK-4000 Roskilde, Denmark

Email: chaoxu@dtu.dk

Abstract. Nucleation of recrystallization near hardness indentations has been investigated in slightly cold rolled high purity aluminium. Samples were cold rolled to 12% and 20% reductions in thickness and indentations were done with two different loads (500 g and 2000 g). The samples were annealed at 300 °C for 1 h and nuclei were identified. It is found that the indentations are preferential nucleation sites. With EBSD maps around indentation tips, the orientation relationship between nuclei and matrix is analyzed. Finally, effects of rolling reduction and indentation load on local misorientations and stored energy distributions and thus on nucleation are discussed.

1. Introduction

Indentation hardness testing of materials is a simple and quick method for obtaining information about the mechanical properties of materials [1], such as yield stress [2, 3] and elastic modulus [4, 5]. In order to understand the mechanisms occurring during indentation better, lots of research of the deformation zones below indentations have been done by different authors [6-10]. A typical early investigation was conducted by Hill et al. [11], who explored the deformation of a plane surface with a wedge and showed that the average strain caused by wedge indentation increases with increasing wedge angle. Further studies investigated the misorientations underneath indents and the dislocation mechanisms explaining the changes within the plastic zone at different indentation depth [12-14] and explored indentation size effects [15-17].

Indentations are also known to provide additional driving force for the nucleation and growth of new grains during annealing. The aim of the present work is to investigate where and how nucleation happens near hardness indents and what orientations the nuclei have. The focus is on the influence of indents load, in cold rolled high purity Al with an initial microstructure coarse enough to do at least one 500 g indentation and one 2000 g indentation within each grain. In this paper, a statistical analysis is made based on all the data obtained from all the grains after annealing. This analysis is referred to as sample scale observation. Furthermore, in order to investigate orientation relationships in more detail, one of the grains is characterized near the indentation tip in the deformed state. This investigation is referred to as local scale observation in the following.

2. Experimental

Two high purity (99.996%) aluminium samples 94 × 46 × 3 mm^3 were used. Initially, they had a coarse and inhomogeneous microstructure with an average grain size of 300 μm. This grain size is too

fine for the planned experiment, therefore all surfaces were ground using 4000# SiC paper and electro polished to prevent nucleation at surface scratches and finally the samples were annealed at 590 °C for 7 days. After annealing, grains with sizes ranging from 500 µm to 7 mm were obtained. These grains are large enough to do several microhardness indents away from the grain boundaries. The samples were cold rolled to 12% and 20% reduction in thickness. Seven samples were cut from them and were carefully ground and electro polished. Microhardness indentations were done on the RD-TD planes using a Vickers diamond indenter of pyramidal shape with loads of 500 g and 2000 g. The distance between each indentation was larger than 3*d*, where *d* is the length of the diagonal lines of the indentations, thereby avoiding deformation zones overlapping. To initiate nucleation, the samples were annealed at 300 °C for 1 h and characterized using electron channeling contrast (ECC) and electron backscattered diffraction (EBSD) with a step size of 2 µm. It should be noted that because of the change in surface position at the indentation, only some scattered pixels can be indexed within the indentation. In order to reveal the indentation-affected zone, one of the cold rolled and indented samples was ground first to reveal the tip of a 500 g indentation and then the sample was ground again to reveal the tip of a 2000 g indentation. After each grinding, the sample was mechanical polished using 40 nm oxide polishing suspension and characterized using EBSD. In all EBSD maps shown in this paper, fine white lines are low angle boundaries (LABs) (≥ 2° and <15°) and coarse black lines are high angle boundaries (HABs) (≥15°).

3. Results and discussion

3.1. Sample scale observations

3.1.1. Nucleation potentials. In total, 57 microhardness indentations were done on six samples and 54 new grains are detected around 28 indentations based on EBSD maps. It should be noted that twins are not counted as recrystallized grains here. For the indentations where we could not be sure if there are nuclei because of only a few indexed pixels at the indents in the EBSD maps, ECC was used to characterize the indentations and an additional 5 nuclei were thereby observed around an additional 4 indentations. Figure 1(a) is an example of using ECC to detect a nucleus that could not be seen by EBSD. Of all the nucleated indentations, most stimulate 1 nucleus except that 8 are found to form 2 nuclei and 8 have 3 or more nuclei. All nuclei have grown into relatively large sizes ranging from tens of micrometres to 300 µm. It should be noticed that no nuclei are detected away from the indentations. This result clearly shows the potentials of indentations to act as nucleation sites, due to the extra driving force provided by the indentation deformation, as suggested in previous investigations [e.g. 13, 14].

(a) (b)

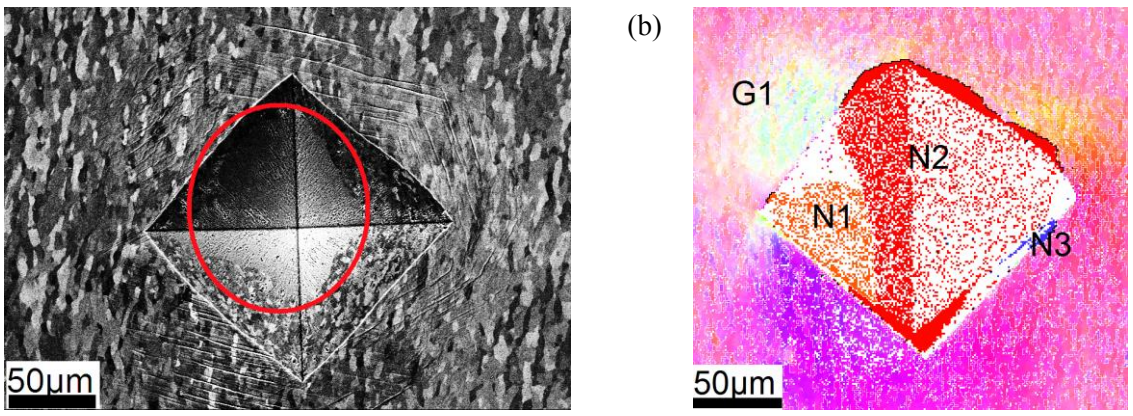

Figure 1. Examples of the nucleation in samples 20% cold rolled and 2000 g indented: (a) an ECC picture showing one nucleus (marked with a red circle) and (b) an EBSD map (without any noise reduction) showing 3 nuclei at another indentation.

The indentations are classified into four types (A, B, C and D) according to the different rolling reductions and different indentation loads, as shown in table 1. The table also reports the total number of indents, and those that have stimulated nucleation. Compared with Type B indentations (20%, 500 g), Type A indentations (20%, 2000 g) have higher nucleation potentials. Similarly, Type D indentations (12%, 500 g) lead to fewer nuclei than Type C indentations (12%, 2000 g). When the samples with 20% rolling reduction (Type A and B) are compared with those less heavily rolled (Type C and D), it is also clear that more nuclei are seen at the indents in the 20% rolled samples (see table 1). These observations clearly show that a higher/larger deformation leads to more nucleation after annealing at 300 °C for 1 hour. It is worth noting that even the most weakly deformed samples (12% rolling and 500 g indentation) can nucleate as was observed when these samples were annealed at 311 °C for 1 h.

3.1.2. Orientation relationships. The microstructures around the 28 nucleated indentations observed using EBSD were analyzed, and the misorientations between each nucleus and the pixel in the neighboring recovered matrix with the smallest misorientation were measured. 11 out of 41 (27%) around Type A indentations have misorientation angles lower than 15° to their neighboring recovered matrix, while for Type B indentations the fraction of the nuclei that have misorientation angles lower than 15° is 33%. One example is shown in figure 1(b). Although only some scattered pixels are detected by EBSD at the indentation surface, we still can in this case clearly distinguish the nuclei, which are numbered as N*i* (*i*=1-3) and the recovered matrix is marked as G1. The boundaries between N1 and G1 are composed of both LABs and HABs. Since some of the boundaries are low angle, N1 is among the 27% of nuclei with orientations near the matrix.

The remaining nuclei, i.e. the 73% nuclei around Type A indentations, 67% nuclei around Type B indentations and the nucleus at Type C indentations, only form HABs with the recovered matrix. For example, both nuclei N2 and N3 only have HABs to the surrounding recovered matrix and no LABs are detected (figure 1(b)). Therefore, one may speculate if this type of nuclei (as N2 and N3) have orientations different from the matrix.

Table 1. Deformation modes and corresponding nucleation at 4 types of indentations

Type	Cold rolling reductions	Loads of indenting	Number of indents	Number of indents with nuclei	Percentage
A	20%	2000 g	18	18	100%
B	20%	500 g	18	13	72%
C	12%	2000 g	10	1	10%
D	12%	500 g	11	0	0

The potentials for growth of nuclei depend on the misorientations between the nuclei and the entire surrounding matrix. Figure 2 shows the distribution of the maximum misorientation angles between the nuclei, which are formed in the 20% cold rolled samples, and their surrounding recovered matrix. It can be observed that the matrix misorientation angles for Type B indentations (load: 500 g) concentrate in the range of 20°~ 30° and do not exceed 35°, while for Type A indentations, the misorientation angles spread widely from 10° to 50°.

3.2. Local scale observations

Although a large fraction of the nuclei as reported above after some growth has orientations different from the observed recovered matrix around the indentations, it does not necessarily mean that these nuclei have been formed with new orientations different from those at the nucleation sites in the deformed matrix. To investigate that, one grain within a 20% cold rolled sample, having the same initial orientation as the example shown in figure 1(b), was chosen to check the deformation microstructure around a 500 g indentation tip and a 2000 g indentation tip in the deformed state.

3.2.1. Local orientation relationship. The microstructures within an area of 85×85 μm^2 around both indentation tips were characterized by EBSD. The {111} pole figure for the microstructures at the indentation of 2000 g is shown in figure 3, where a large orientation spread in the deformed matrix around the indentation tip is revealed as grey clouds. As the selected deformed grain has the same orientation as that annealed and shown in figure 1(b), the orientations of the nuclei N1-N3 are also plotted in figure 3 as large crosses, circles and diamonds, respectively. When comparing these orientations with the orientation spread at the indentation tip in the deformed state (grey cloud in figure 3), it is clear that N1 (marked by diamonds) has an orientation well within the deformed orientation spread, while N2 (marked by circles) and N3 (marked by crosses) both are at the outskirts but yet within the orientation spread in the deformed state. It is thus very likely that these 3 nuclei had nucleated from the sites in the deformed matrix with the actual orientation around the indentation tip, i.e. they formed with an orientation within the spread of the deformed matrix and grew to meet new areas with different orientations, thereby forming high angle boundaries (and as N2 and N3, they grew to belong to the large fraction of nuclei which had a minimum misorientation to the surrounding recovered matrix of above 15°).

It is clear that the indentations lead to significant extra deformation and consequently extra orientational scatter which has to be considered when studying nucleation. This is investigated in detail for both the 500 g and the 2000 g indentation in the following.

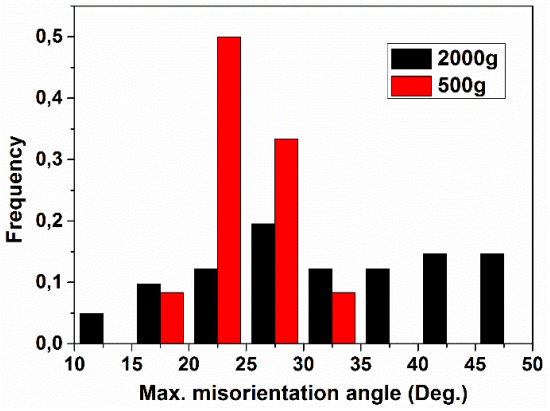

Figure 2. Maximum misorientation between nuclei and the surrounding pixels in the recovered matrix. The red and black histograms represent the data for the 500 g and the 2000 g indentations in the 20% cold rolled samples, respectively.

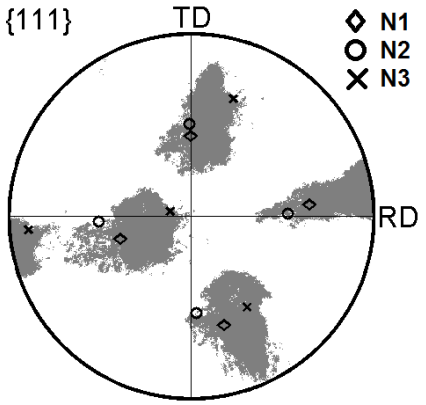

Figure 3. {111} pole figure showing the orientations within an area of 85×85 μm^2 around the tip of a 2000 g indentation in the deformed state of the 20% cold rolled sample. The grey cloud represents the orientations of the deformed matrix.

3.2.2 Microstructure and stored energy. In figure 4(a) and (b), the measured orientations are shown and the figures reveal the largely symmetric distributions of orientations given by the pyramidal shape of the indenter. The orientation distributions caused by the indenter may also be visualized with respect to the orientation in the 20% rolled matrix away from the indentation. This is shown in figure 4(c) and (d). In these figures, the matrix away from the indentation has more or less the same orientation and thus is shown in blue i.e. with misorientations below 15°. Most of the indentation zone both after 500 g and 2000 g load is rotated between 10° and 30° away from the matrix, and shown in green in figure 4(c) and (d). Small local zones near the tip and along a symmetry axis, however, have misorientations to the matrix above 35°; most pronounced after the 2000 g indentation where a series of misorientation peaks above 40° are seen along a symmetry axis (see figure 4(d)). Such peaks are expected to be powerful nucleation sites, leading to nuclei with orientations far away from the matrix orientations. The largest rotation angles of ~50° and ~35° under the 2000 g and 500 g indentations,

respectively, agree well with the observed maximum misorientations between nuclei and the surrounding matrix shown in figure 2.

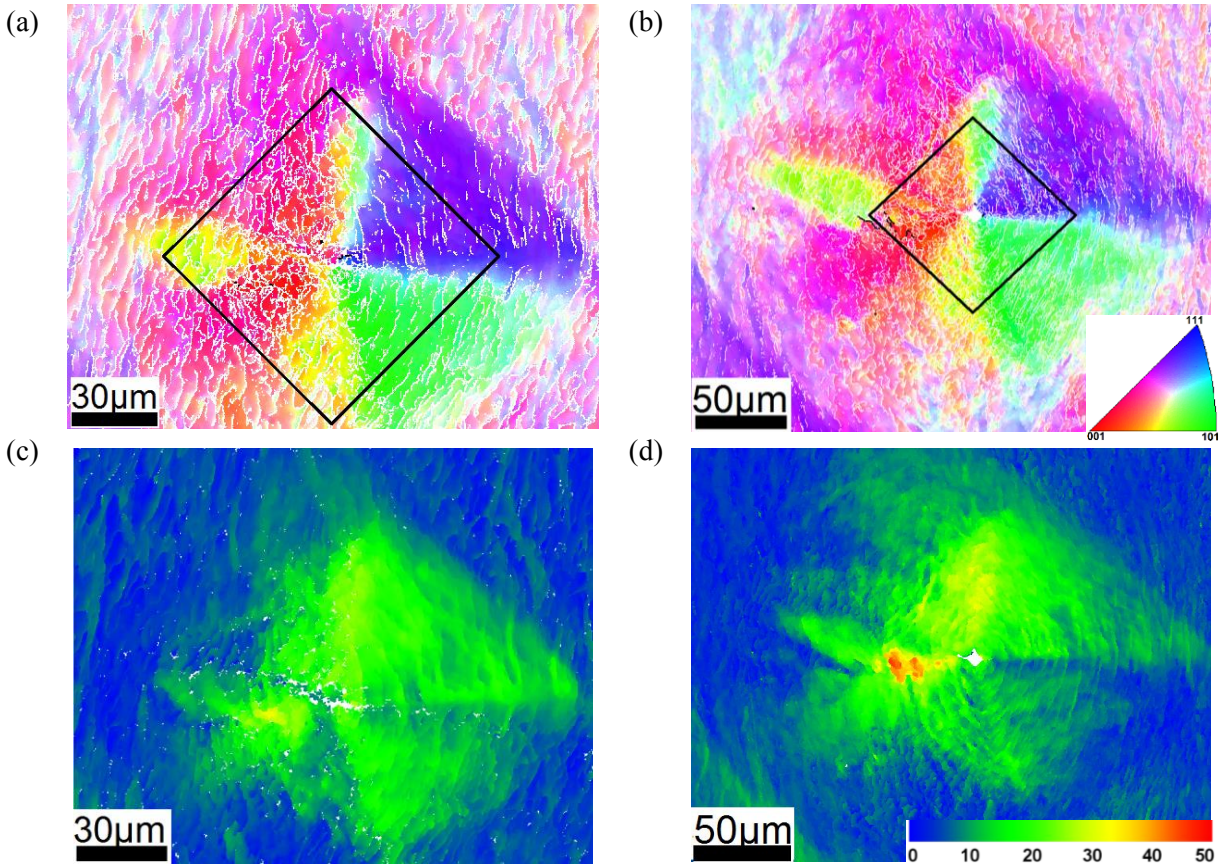

Figure 4. The deformation microstructures around a 500 g indentation (a, c) and a 2000 g indentation (b, d) in a 20% cold rolled sample. The color in (a) and (b) is defined by inverse pole figure color and the color in (c) and (d) is based on the misorientation angle between each pixel and the orientation in the 20% rolled matrix away from the indentation. The two diamonds in (a) and (b), which have the same size of 120 µm along the diagonals are used for direct comparison of stored energies. For the 500 g indentation, the size of the diamond is chosen to almost cover the region with a large misorientation (the green area in (c)).

The extra driving force introduced by the indentations may be estimated as stored energy (SE) from the measurements shown in figure 4(a) and (b). Such estimation is based on the measured misorientations across deformation-induced boundaries which can be obtained from EBSD data using a method described in [18], including all boundaries with misorientation ≥2°.

For this estimation an area near the tip is used (marked by the diamond in figure 4(a) and (b)). The size of the area is chosen to be the same for the 500 g and 2000 g indents to allow a direct comparison of SE at this central indentation zone in the two cases. The calculated results are 0.12 MJ/m^3 and 0.15 MJ/m^3 for the 500 g and 2000 g indentations, respectively. The SE in an area of the same size away from the indentation is only 0.04 MJ/m^3.

It has to be noted that the present analysis is based on 2D measurements which leads to uncertainties in the calculation of SE. Furthermore, with EBSD and ECC techniques it is not possible to follow the nucleation in-situ away from the polished surface. Therefore it is not possible to pin point the exact nucleation sites in the deformed matrix. Only by non-destructive 3D measurements, e.g. by synchrotron X-rays, it would be possible to overcome these limitations.

4. Conclusions

High purity very coarse grained Al was used to investigate effects of indenting loads and rolling reductions on recrystallization nucleation. It was found that the indentations lead to substantial additional grain subdivision of the deformed microstructure and large orientation rotations near the indentation tips. The higher the indentation loads the larger are the subdivision and additional SE. For indentations with a 500 g load, high angle boundaries with up to 25° misorientation are formed, local zones with misorientation up to 35° away from the matrix are observed and the additional SE near the tip is 0.08 MJ/m^3. The numbers for a 2000 g load are 25°, 50° and 0.11 MJ/m^3 respectively. It is thus not surprising that nucleation occurs near the indentation. No nuclei are observed away from the indentations. The higher the indentation load, the more nuclei. However, also the rolling reduction contributes here. Whereas the majority (>70%) of the indentations in the 20% cold rolled samples lead to nucleation, only 1 indentation out of 21 causes detectable nucleation in the 12% cold rolled samples at the chosen annealing condition (300 °C for 1 h). By local orientation measurements near the indentation tip in the deformed state, it is shown that the orientational spread observed there covers the orientations of the nuclei observed in the annealed state of an identical sample. It is thus suggested that the nuclei form at local sites in the indentation zone with orientations as those present there and will have large misorientations to the rolled matrix, into which they grow after some annealing.

Acknowledgements

CLX, GLW and QL gratefully acknowledge the support from the NSFC of China (Grant No. 51471039, 51327805 and 51421001) and Fundamental Research Fund of Central Universities (Grant No. 10611205CDJZXZ138802). All Authors wish to thank the support from the Danish National Research Foundation (Grant No.DNRF86-5) and the NSFC of China (Grant No. 51261130091) to the Danish-Chinese Center for Nanometals. Helpful discussions with and suggestions from Jun Sun and Xuehao Zheng are grateful acknowledged.

References

[1] Tabor D 1951 *The hardness of Metals*, Oxford, UK, Oxford University Press
[2] Clausner A and Richter F 2015 *Eur. J. Mech. A/Solid* **51** 11-20
[3] Kramer D, Huang H, Kriese M, Robach J, Nelson J, Wright, Bahr D and Gerberich WW 1999 *Acta Mater.* **47** 333-43
[4] Hu Z, Lynne K J, Markondapatnaikuni S P and Delfanian F 2013 *Mater. Sci. and Eng. A* **587** 268-82
[5] Vandeperre L J and Clegg W J 2005 *Acta Mater.* **492-493** 555-60
[6] Mulhearn T O 1959 *J. Mech. Phys*. **7** 85-96
[7] Keh A S 1960 *J. Appl. Phys.* **31** 1538-45
[8] Inkson B J, Steer T, Mobus G, Wabner T 2000 *J. Microsc-oxford* **201** 256-69
[9] Mogilecsky P 2005 *Philos. Mag.* **85** 3511-39
[10] Rester M, Motz C and Pippan R 2007 *Acta Mater.* **55** 6427-35
[11] Hill R, Lee E H and Tupper S J 1947 *Proc. R. Soc. A.* **188** 273-89
[12] Kiener D, Pippan R, Motz C and Kreuzer H 2006 *Acta Mater.* **54** 2801-11
[13] Xie G, Wang L, Zhang J and Lou L H 2012 *Scripta Mater.* **66** 378-81
[14] Zambaldi C, Rosters F, Raabe D and Glatzel U 2006 *Mater. Sci. Eng. A* **454-455** 433-40
[15] Demir E, Raabe D, Zaafarani N and Zaefferer S 2009 *Acta Mater.* **57** 559-69
[16] Nix W D and Gao H 1998 *J. Mech. Phys. Sol.* **46** 411-25
[17] Begley M R and Hutchinson J W 1998 *J. Mech. Phys. Sol.* **46** 2049-68
[18] Godfrey A, Cao W Q, Liu Q and Hansen N 2005 *Metall. Mater. Tran. A* **35** 2371-78